Cell Host & Microbe
Article

A *Pseudomonas syringae* Effector Inactivates MAPKs to Suppress PAMP-Induced Immunity in Plants

Jie Zhang,[1,3] Feng Shao,[3] Yan Li,[3] Haitao Cui,[3] Linjie Chen,[3] Hongtao Li,[3] Yan Zou,[3] Chengzu Long,[3] Lefu Lan,[2] Jijie Chai,[3] She Chen,[3] Xiaoyan Tang,[2] and Jian-Min Zhou[3,*]
[1] National Key Laboratory of Plant Molecular Genetics, Institute of Plant Physiology and Ecology, Shanghai Institutes for Biological Sciences, Chinese Academy of Sciences, Shanghai 200032, China
[2] Department of Plant Pathology, Kansas State University, Manhattan, KS 66506, USA
[3] National Institute of Biological Sciences, Beijing 102206, China
*Correspondence: zhoujianmin@nibs.ac.cn
DOI 10.1016/j.chom.2007.03.006

SUMMARY

Pathogen-associated molecular patterns (PAMPs) elicit basal defense responses in plants, and, in turn, pathogens have evolved mechanisms to overcome these PAMP-induced defenses. To suppress immunity, the phytopathogenic bacterium *Pseudomonas syringae* secretes effector proteins, the biochemical function and virulence targets of which remain largely unknown. We show that HopAI1, an effector widely conserved in both plant and animal bacterial pathogens, inhibits the *Arabidopsis* mitogen-activated protein kinases (MAPKs) activated by exposure to PAMPs. HopAI1 inactivates MAPKs by removing the phosphate group from phosphothreonine through a unique phosphothreonine lyase activity, which is required for HopAI1 function. The inhibition of MAPKs by HopA1 suppresses two independent downstream events, namely the reinforcement of cell wall defense and transcriptional activation of PAMP response genes. The MAPKs MPK3 and MPK6 physically interact with HopAI1 indicating that they are direct targets of HopAI1. These findings uncover a mechanism by which *Pseudomonas syringae* overcomes host innate immunity to promote pathogenesis.

INTRODUCTION

Plants are known to activate defenses in response to nonspecific elicitors from diverse microbes (Boller, 1995). Studies in both animal and plant innate immunity in recent years have indicated that these elicitors constitute pathogen-associated molecular patterns (PAMPs), triggering basal defenses in the host (Nürnberger and Lipka, 2005; Zipfel and Felix, 2005). Because PAMPs also exist in nonpathogenic microbes, they have also been referred to as microbe-associated molecular patterns (MAMPs; Ausubel, 2005). PAMP-triggered plant defenses form a formidable layer of resistance deterring numerous potential pathogens (Kang et al., 2003; Li et al., 2005). An emerging consensus is that pathogens infecting the modern day land plants have evolved mechanisms to overcome the PAMP-induced defenses in their respective host plants (Chisholm et al., 2006). Therefore, PAMP-triggered defenses are at the core of understanding both plant disease resistance and bacterial pathogenicity.

The best understood PAMP of plant pathogens is arguably flg22, a conserved peptide derived from *Pseudomonas syringae* flagellin (Felix et al., 1999). Flg22 is perceived by the receptor kinase FLS2 in *Arabidopsis* to stimulate cell wall defenses exemplified by callose deposition (Felix et al., 1999; Gomez-Gomez and Boller, 2000), ethylene production (Felix et al., 1999; Liu and Zhang, 2004), and reprogramming of transcriptome (Zipfel et al., 2004; Navarro et al., 2004; Thilmony et al., 2006). Immediately after the exposure to flg22, plants activate a rapid but transient oxidative burst (H_2O_2 production; Felix et al., 1999) and mitogen activated protein kinases (MAPKs) MPK3 and MPK6 (Asai et al., 2002). However, it is not known if a causal relationship exists between MAPK activation and oxidative burst.

Gram-negative bacteria use a specialized type III secretion system to deliver a repertoire of effector proteins into host cells to subvert host immunity, thereby promoting parasitism (Alfano and Collmer, 2004). Several plant proteins are known to interact with *P. syringae* effectors (Mackey et al., 2002; Axtell and Staskawicz, 2003; Mackey et al., 2003; Shao et al., 2003; Nomura et al., 2006). However, thus far only one of these, an immunity-associated protein in *Arabidopsis thaliana*, is known to be targeted by the bacterial effector to mediate virulence (Nomura et al., 2006). In addition, we have only rudimentary knowledge of PAMP-signaling mechanisms, all of which has impeded our understanding of bacterial virulence mechanisms.

We have shown previously that the *P. syringae* HopAI1 protein belongs to an effector family widely conserved in both animal and plant pathogenic bacteria (Li et al., 2005). Supporting an important role of this effector family in infection, the *Salmonella typhimurium* effector SpvC, a HopAI1 family member, is required for bacterial virulence in mice (Gulig and Chiodo, 1990). Expression of HopAI1 in

plants enhances disease susceptibility to *P. syringae* and suppresses flg22-induced transcription of *Arabidopsis NHO1*, a gene required for basal resistance to *P. syringae* (Kang et al., 2003; Li et al., 2005). These results indicate that HopAI1 targets the PAMP-mediated signaling to suppress host defenses. The biochemical function and host target of HopAI1 and its family members remain unknown.

Here we show that HopAI1 directly inactivates MPK3 and MPK6 by dephosphorylation and consequently suppresses flg22-induced gene expression, oxidative burst, and callose deposition, resulting in increased disease susceptibility in plants. We recently found that the *Shigella* effector OspF, a HopAI1 family member, cleaves the C-OP bond at the phosphothreonine residue of animal MAPK (Li et al., 2007). HopAI1 carries the same activity to remove the phosphate group from phosphothreonine of *Arabidopsis* MAPKs. Mutational analysis indicates that this enzymatic activity is required for HopAI1 to suppress flg22-triggered MAPK activation and immune responses.

RESULTS

hopAI1 Contributes to *Pseudomonas syringae* pv. *tomato* Virulence in Plants

The *hopAI1* genes carried by the two previously known *Pseudomonas* strains *P.s.* pv. *tomato* DC3000 and *P.s.* pv. *syringae* B728A appear to be inactive (Lindeberg et al., 2006; Vinatzer et al., 2006). To determine if *hopAI1* is a functional gene in any *Pseudomonas* strains, we surveyed 26 strains for sequences crosshybridizing the *P.s.* pv. *tomato* DC3000 *hopAI1.* All 14 *P. syringae* pv. *tomato* strains tested contained *hopAI1* sequence (Figure S1A), suggesting that *hopAI1* plays an important role in *P. syringae.* pv. *tomato. P.s.* pv. *tabaci* R1152 race 0 and *P.s.* pv. *glycinea* race 0 contained clear but weaker hybridizing sequences, suggesting the presence of homologous sequences (Figure S1A). In contrast, other strains did not carry homologous sequences. Northern analysis was used to determine if any of the *P. syringae.* pv. *tomato* strains carried an active *hopAI1* gene. At least two *P.s.* pv. *tomato* strains, 0288-9 and 0488-5, actively transcribed *hopAI1* mRNA in the minimal medium that is known to induce *P. syringae* type III effectors (Figure S1B).

To determine if HopAI1 plays a role in bacterial virulence, we generated a knockout mutant in strain 0288-9 by using homologous recombination. Because 0288-9 is only modestly virulent on *Arabidopsis* but highly virulent on tomato plants, we tested the ability of the mutant strain to grow in tomato plants. The mutant bacteria consistently multiplied to a lower level compared with WT bacteria (Figure 1A). The difference is statistically significant (Student's t test, p value ≤ 0.01), indicating a positive role of *hopAI1* in 0288-9 virulence.

HopAI1 Suppresses Both PAMP-Induced Gene Expression and Callose Deposition

Previously we showed that estrogen-inducible expression of a FLAG-tagged *HopAI1* transgene in plants enhanced susceptibility to a nonpathogenic *P. syringae* mutant (Li et al., 2005), suggesting a loss of PAMP-induced resistance. We examined flg22-induced disease resistance in plants expressing HopAI1. Pretreatment of flg22 protects *Arabidopsis* plants from a subsequent infection by virulent bacteria (Zipfel et al., 2004). While the flg22-pretreatment completely inhibited the multiplication of the virulent *P. syringae* strain DC3000 in the wild-type plants, the same treatment did not protect in the HopAI1-expressing plants (Figure 1B), indicating that HopAI1 completely suppresses disease resistance activated by flg22.

To understand the function of HopAI1 in plants, we sought to characterize in detail the flg22-induced gene expression and callose deposition when HopAI1 is directly expressed in plants. Figure S2A shows that transient expression of a FLAG-tagged HopAI1 in protoplasts blocked the flg22-induced expression of the *FRK1-LUC* reporter gene. *FRK1* encodes a receptor-like kinase that is induced rapidly in response to PAMPs (Asai et al., 2002). The suppression is not caused by a general disruption of cellular activities, because HopAI1 does not affect the *LUC* reporter gene expression under the control of the CaMV 35S promoter (Figure S2B). We further expanded this study in *HopAI1* transgenic plants by examining the expression of flg22-inducible genes including *FRK1*, *WRKY22*, *WRKY29*, *At1g13110*, *At1g30700*, *At2g35930*, *At2g39200*, *At5g39580*, and *At5g44910* (Asai et al., 2002; http://Arabidopsis.org/info/expression/ATGenExpress.jsp). These genes encode functionally diverse proteins and serve as a good survey of gene expression profiles. The expression of HopAI1 reduced flg22-induced expression of all genes tested (Figures 1C). The stronger suppression of flg22-induced genes by HopAI1 in protoplasts than transgenic plants might be caused by higher-level HopAI1 expression associated with this transient assay. The estradiol-inducible expression of HopAI1 also blocked flg22-induced callose deposition (Figure 1D). PAMP-induced callose deposition is required for *Arabidopsis* resistance to *P. syringae* bacteria (Kim et al., 2005). These analyses indicated that the plant-expressed HopAI1 broadly suppresses flg22-induced defenses.

HopAI1 Suppresses Early Signaling Events

The suppression of callose deposition and defense gene expression suggested that HopAI1 targets an early step of the PAMP-induced signaling pathway. We thus tested the effect of HopAI1 on two known signaling events: MAPK activation and transient oxidative burst, both occurring within less than 5 min after flg22 stimulation. Consistent with the previous report (Felix et al., 1999), wild-type plants treated with flg22 displayed a rapid and transient accumulation of H_2O_2 within 5 min (Figure 2A), whereas the *fls2* mutant displayed no detectable production of H_2O_2 (data not shown). The estradiol-induced expression of HopAI1 in plants completely abolished flg22-induced accumulation of H_2O_2. The flg22-treatment increased MAPK activities attributed to MPK3 and MPK6, as indicated by the lack of corresponding activities in

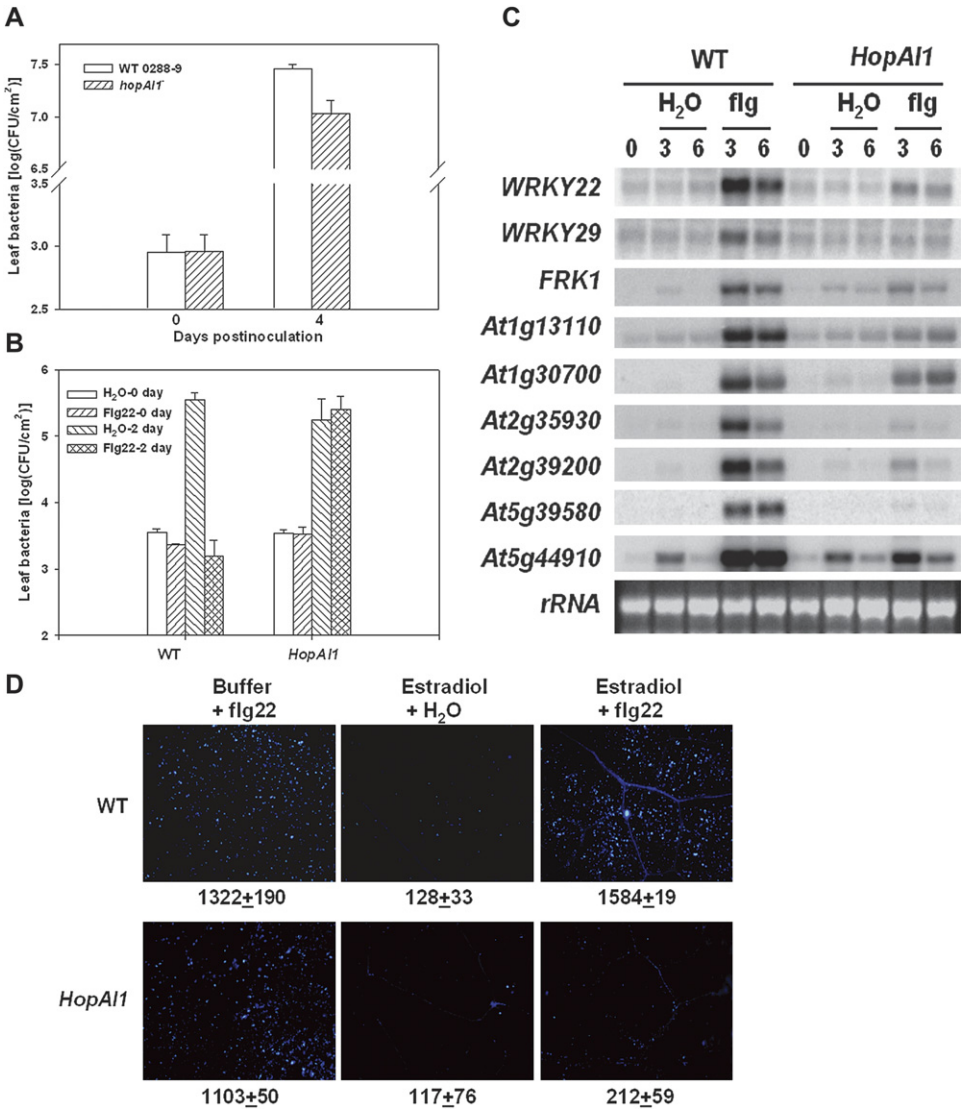

Figure 1. HopAI1 Contributes to Bacterial Virulence and Abolishes Flg22-Induced Resistance by Globally Suppressing Defenses

(A) *HopAI1* is required for full virulence of *P.s.* pv. *tomato* strain 0288-9. Tomato plants were infiltrated with the WT or *hopAI1*$^{-}$ mutant bacteria (10^5 CFU/ml), and leaf bacterial population was determined at the indicated times. Error bars indicate standard deviation. The experiment was done twice with similar results.

(B) Expression of HopAI1 abolishes flg22-induced resistance to *P. syringae.* Wild-type (WT) and *HopAI1* transgenic plants were presprayed with estradiol or H_2O for 12 hr, infiltrated with 1 μM flg22 or H_2O for one day, and infiltrated with *P. syringae* DC3000 bacteria. Each data point consisted of at least four replicates. Error bars indicate standard deviation. Two independent experiments were performed with similar results.

(C) HopAI1 suppresses flg22-induced gene expression. WT and *HopAI1* transgenic plants were presprayed with estradiol for 24 hr before infiltrated with H_2O or 1 μM flg22 (flg) for the indicated times, and RNA was extracted for northern analyses using the indicated probes. A representative ethidium bromide stain is shown for equal loading of RNA. The experiment was repeated three times with similar results.

(D) HopAI1 suppresses flg22-induced callose deposition. WT and *HopAI1* transgenic plants were presprayed with estradiol or H_2O, treated with flg22, and leaves were stained with alanine blue for callose. Microscopic photographs of callose deposits were shown with number of callose deposits indicated below each photograph. Error bars indicate standard deviation. The results are a representative of five independent experiments.

atmpk3 and *atmpk6* mutants (Figure 2B). The expression of HopAI1 completely abolished both MPK3 and MPK6 activities (Figure 2B). The diminished MAPK activity was not caused by a reduced MPK3 and MPK6 protein levels as indicated by western analysis (Figure 2B). Transient expression of HopAI1 in protoplasts also abolished flg22-induced MAPK activity (see below). These results are surprising, as a recent paper by He et al. (2006) reported that HopAI1 does not inhibit MAPKs. An examination of the annotated *hopAI1* sequence suggested that the discrepancy might be caused by an extra N-terminal sequence (Figure S3A) present in our construct but missing in the

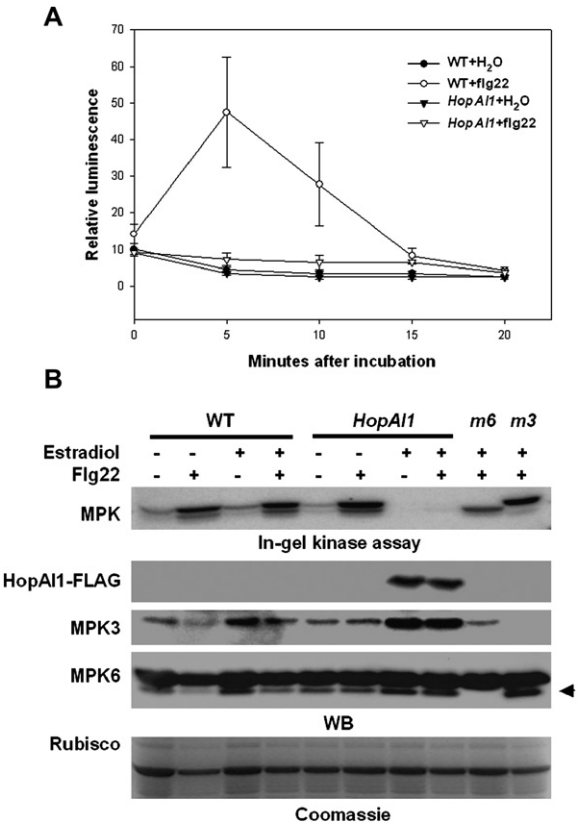

Figure 2. HopAI1 Acts Very Early to Suppress PAMP Signaling

(A) HopAI1 suppresses flg22-induced oxidative burst. WT and *HopAI1* transgenic plants were presprayed with estradiol or H_2O. Leaf strips were then treated with flg22, and H_2O_2 accumulation was measured (expressed as relative units of luminescence). Error bars indicate standard deviation. The experiments were repeated 3 times with similar results.

(B) HopAI1 suppresses PAMP-triggered activation of MPK3 and MPK6. WT, *HopAI1* transgenic, and the *atmpk6* (*m6*) and *atmpk3* (*m3*) mutant plants (carrying T-DNA insertions in respective genes) were presprayed with H_2O (−) or estradiol, treated with flg22 for 10 min, and protein was extracted for in-gel kinase assay using myelin basic protein as a substrate. Equal amounts of extracts were also subjected to western blot analysis using anti-FLAG, anti-MPK3, and anti-MPK6 antibodies. The arrow indicates the position of MPK6. The amounts of protein loaded are indicated by the Coomassie Blue staining of Rubisco.

annotated sequence and the construct used by He et al. (2006). Because this sequence is highly conserved in all the HopAI1 family members in various bacteria, the predicted amino acid sequence in the *P. syringae* database is likely annotated incorrectly. To determine if the N-terminal sequence is required for the activity, an N-terminal truncated construct (ΔNHopAI1) lacking this sequence was generated and expressed in protoplasts. However, ΔNHopAI1 still abolished the flg22-induced MAPK activity (Figure S3B), indicating that this N-terminal sequence is dispensable for MAPK inhibition. In total, we conducted 8 independent assays with transgenic HopAI1 plants and 8 assays with protoplasts expressing sequence-confirmed full-length (3 clones) and ΔNHopAI1 (2 clones) constructs. In each case, the flg22-induced MAPK activity was abolished. We thereby conclude that HopAI1 inhibits the MAPK activation. The suppression of oxidative burst and inhibition of MAPK indicate that HopAI1 targets a very early step in the PAMP-signaling pathway to block host defenses.

MAPKs Act Upstream of Oxidative Burst

It was proposed that ROI produced during oxidative burst might act upstream to activate MAPKs (Kovtun et al., 2000). It is therefore possible that HopAI1 targets a host protein(s) required for oxidative burst that consequently inhibits MAPK. Alternatively, MAPK may act upstream of ROI production.

To determine if oxidative burst acts upstream of MAPK activation, we first determined the source of ROI production in flg22-induced tissues. In plants, NADPH oxidases, peroxidases, and ROI scavenging systems can all contribute to the increase of ROIs in response to pathogen infection (Torres et al., 2006). *Arabidopsis* contains 10 genes encoding NADPH oxidases named respiratory burst oxidase homologs (*Atrboh;* Torres and Dangl, 2005). The *AtrbohD* and *AtrbohF* are required for ROI production in plants challenged with incompatible pathogens (Torres et al., 2002). A recent study shows that ROIs produced by *AtrbohD* and *AtrbohF* suppress cell death (Torres et al., 2005). Whether these two genes play a role in PAMP-induced defenses has not been examined. We therefore tested if they are required for ROI production in response to flg22. In contrast to the strong accumulation of H_2O_2 in the wild-type plants, the *atrbohD* mutant was completely impaired in this oxidative burst (Figure 3A). The *atrbohF* mutant showed a minor reduction in H_2O_2 accumulation. The results indicated that *AtrbohD* is essential for flg22-induced oxidative burst, whereas *AtrbohF* plays a minor role.

The flg22-induced callose deposition was examined in the *atrbohD* mutant plants. In contrast to the strong flg22-induced callose deposition in the wild-type plants, the *atrbohD* mutant exhibited significantly reduced callose deposition (approximately 16% of the wild-type; Figure 3B), suggesting that the AtrbohD-dependent ROI production mediates callose deposition. Consistent with this possibility, pretreatment of the wild-type plants with diphenylene iodonium (DPI), a NADPH oxidase inhibitor, abolished the flg22-induced callose deposition (Figure S4). Together these results demonstrated that AtrbohD ROI regulates cell wall defense exemplified by callose deposition.

We next determined if flg22-induced gene expression was compromised in the *atrbohD* mutant by northern analysis. Interestingly, both the wild-type and *atrbohD* mutant plants showed normal induction of all genes tested (Figure S5). As several of these genes are induced downstream of MPK3 and MPK6 (He et al., 2006), the results suggest that AtrbohD is not required for MAPK activation. Indeed, the flg22-induced MAPK activation was completely normal in the *atrbohD* mutant (Figure 3C), indicating that the AtrbohD-dependent ROI production is either

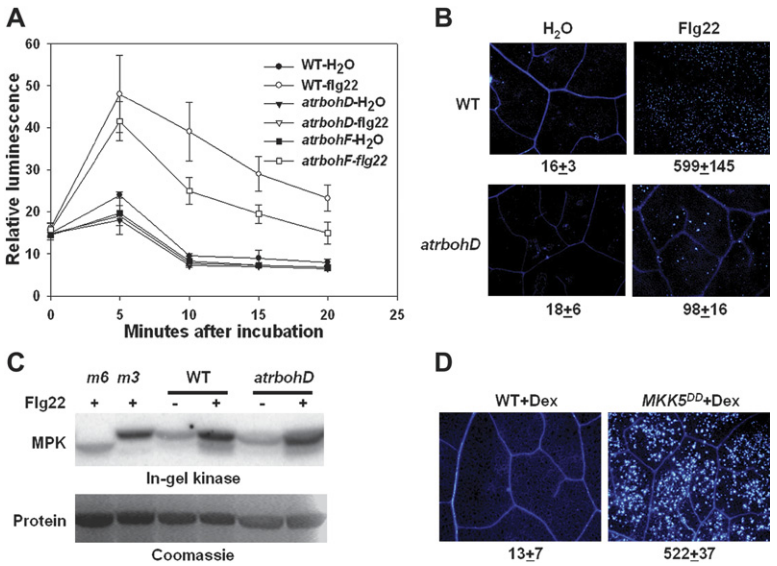

Figure 3. MAPKs Act Upstream to Regulate the AtrbohD-Mediated Oxidative Burst and Callose Deposition

(A) The *atrbohD* mutant is impaired in flg22-induced H_2O_2 production. Leaf strips from WT, *atrbohD*, and *atrbohF* plants were treated with 1 μM flg22 or H_2O, and the production of H_2O_2 was measured at the indicated times. Each time point consisted of at least 6 replicates. Error bars indicate standard deviation. The experiment was repeated 4 times with similar results.

(B) *atrbohD* diminishes flg22-induced callose deposition. Error bars indicate standard deviation. The experiment was repeated 4 times with similar results.

(C) MAPKs are activated normally in the *atrbohD* mutant. Plants were stimulated with flg22, and extracts were subjected to in-gel kinase assay.

(D) Activation of MAPKs is sufficient to induce callose deposition. Transgenic $MKK5^{DD}$ plants were induced with 30 μM Dex for 24 hr before callose staining. Error bars indicate standard deviation.

too low or too transient to activate MAPKs. These analyses indicated that AtrbohD is only required for a subset of defenses. Consistent with this conclusion, the *atrbohD* mutant is partially compromised in flg22-induced disease resistance as determined by flg22-protection assay (Figure S6). Together these results suggested that the AtrbohD-dependent ROI production occurs either downstream or independent of MAPK activation.

If MPK3 and MPK6 act upstream of AtrbohD ROI, the activation of these MAPKs is expected to induce callose deposition in the absence of PAMPs. We therefore tested if constitutive activation of MPK3 and MPK6 by the constitutive active MKK5 ($MKK5^{DD}$; Liu and Zhang, 2004) is sufficient to induce callose. Indeed, expression of $MKK5^{DD}$ under the control of a dexmethasome (Dex)-inducible promoter resulted in strong callose deposition in the absence of PAMPs (Figure 3D). Because constitutive activation of MPK3 and MPK6 by MKK5 is known to induce the transcription of flg22-inducible genes including *FRK1, WRKY22* and *WRKY29*, it is evident that MPK3 and MPK6 are responsible for both cell wall defenses and gene regulation. We therefore conclude that MAPKs act upstream of AtrbohD, with the latter mediating the cell wall defense pathway.

HopAI1 Directly Targets MPK3 and MPK6

The analyses described above raised the possibility that HopAI1 act directly on components of the MAPK cascade. Because MPK3 and MPK6 can be activated by the expression of constitutive active form of MEKK1 (ΔMEKK1; Asai et al., 2002) or $MKK5^{DD}$ (Liu and Zhang, 2004), we expressed ΔMEKK1 and $MKK5^{DD}$ mutants in protoplasts and tested MAPK activation. Coexpression of HopAI1 abolished MAPK activity triggered by constitutive expression of either ΔMEKK1 or $MKK5^{DD}$ (Figure 4A, left panel). Furthermore, MAPK activation in protoplasts carrying the Dex-inducible MKK^{DD} transgene was also abolished when HopAI1 was coexpressed (Figure 4A, right panel). In contrast, the expression of AvrPto that is known to act upstream of MEKK1 (He et al., 2006) did not affect MAPK activation by ΔMEKK1 or $MKK5^{DD}$ (Figure 4A). Together these results demonstrated that HopAI1 acts on or downstream of an MKK, either by directly targeting MPK3 and MPK6 or by preventing the phosphorylation of MPK3 and MPK6 by the upstream MKK.

Protein pull-down assay was carried out to determine if HopAI1 directly binds MPK3 and MPK6 in vitro. GST-HopAI1 was coexpressed with His-tagged MPK3 or MPK6 in *E. coli*, purified with glutathione agarose, and the pull-down products were tested for the presence of MPK3 or MPK6 with western blot. GST-HopAI1, but not GST alone, copurified with MPK3 and MPK6 (Figure 4B), indicating a direct interaction between HopAI1 and the two MAPKs. Coimmunoprecipitation was used to verify if such an interaction occurs in vivo. Protein extracts expressing HopAI1-FLAG was precipitated with an argorse-conjugated anti-FLAG monoclonal antibody. Subsequent western blot analysis detected MPK3 and MPK6 in the immune complex (Figure 4C). The results demonstrated that HopAI1 directly targets MPK3 and MPK6.

HopAI1 Is a Phosphothreonine Lyase that Inactivates MAPKs

To elucidate the mechanism by which HopAI1 inhibits MAPKs, we tested if the MAPKs activated by the flg22-treatment can be inactivated by the recombinant HopAI1 protein. The core fragment $HopAI1^{7-245}$ (lacking the N-terminal 6 amino acids that are not required for function and the C-terminal 22 amino acids that are not conserved in the HopAI1 family) was used for optimum stability and purity. Total protein extracts from flg22-activated

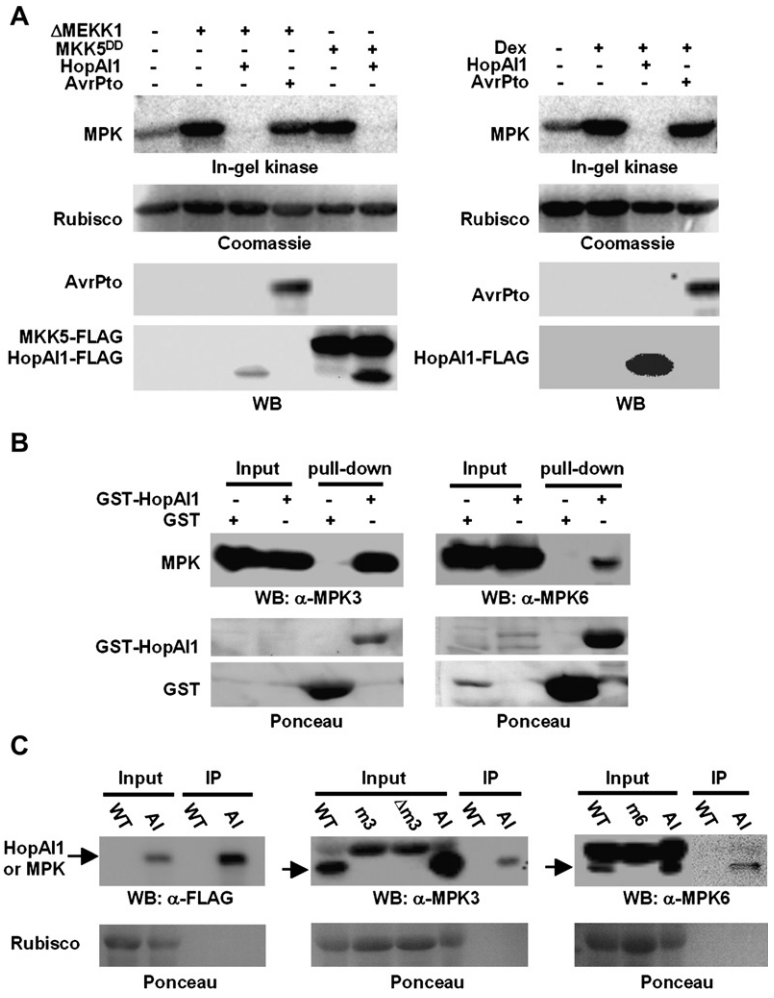

Figure 4. HopAI1 Directly Targets MPK3 and MPK6

(A) HopAI1 inhibits MAPKs downstream of MEKK and MKK. Left: Protoplasts were transfected with ΔMEKK1 or MKK5^{DD} alone or in combination with HopAI1 or AvrPto before protein extraction. Right: Protoplasts prepared from Dex-inducible MKK5^{DD} transgenic plants were transfected with HopAI1 or AvrPto, induced with Dex before in-gel kinase assay. The amount of protein loaded is indicated by Coomassie Blue staining. The level of AvrPto, HopAI1-FLAG and MKK5-FLAG was determined by western blot analysis using anti-AvrPto and anti-FLAG antibodies. The experiment was repeated twice with similar results.

(B) HopAI1 directly interacts with MPK3 and MPK6 in vitro. GST-HopAI1 were coexpressed with His-MPK3 or MPK6-His in *E. coli*, precipitated with glutathione agarose, and western blot analysis was used to detect the presence of MPK3 or MPK6. His-MPK3 and MPK6-His coexpressed with GST were used as control for specific interactions. Amounts of protein loaded are indicated by Ponceau S staining. The results shown are representative of two independent experiments.

(C) HopAI1 interacts with MPK3 and MPK6 in vivo. WT, T-DNA insertional mutants *atmpk3* (*m3*) and *atmpk6* (*m6*), a fast neutron-generated *atmpk3* deletion mutant (*Δm3*), and *HopAI1* (*AI*) transgenic plants were treated with 50 μM estradiol for 12 hr. Soluble protein was extracted and precipitated with an agarose-conjugated anti-FLAG monoclonal antibody. The presence of HopAI1-FLAG, MPK3, and MPK6 in the immunocomplex was detected with the indicated antibodies. Two independent experiments were done with similar results.

tissues were incubated with the purified recombinant HopAI1$^{7-245}$ protein (with GST removed) prior to in-gel kinase assays. Incubation of the extracts with HopAI1$^{7-245}$ for 20 min completely abolished the MAPK activity, whereas the incubation with BSA did not (Figure 5A). Significant reduction of the MAPK activity was observed within less than 30 s of incubation with HopAI1 (Figure 5A, left panel). As little as 20 ng HopAI1 was needed to significantly reduce the MAPK activity (Figure 5A, right panel). Because HopAI1$^{7-245}$ and the MAPKs were separated in the denaturing gel prior to the activity assay, the lack of MBP phosphorylation is indicative of a covalent inactivation of MPK3 and MPK6 by HopAI1, most likely by the removal of phosphate groups required for MAPK activity. To test this possibility, we used recombinant MKK5^{DD}-His protein to phosphorylate GST-MPK3 and GST-MPK6. The phosphorylated MAPKs were then treated with the purified HopAI1$^{7-245}$ protein or BSA, and the level of dual phosphorylation of the TXY motif of MAPKs was detected with anti-phospho-ERK antibodies. Figure 5B shows that the amounts of phosphorylation in both MPK3 and MPK6 were significantly reduced in the presence of HopAI1$^{7-245}$, but not BSA. Together, these results demonstrated that HopAI1 inactivates MAPKs by dephosphorylation. To further investigate the enzymatic activity of HopAI1 in dephosphorylating MAPKs, a synthetic MPK6 phosphopeptide carrying p-threonine and p-tyrosine at the TXY motif was incubated with recombinant HopAI1$^{7-245}$, and the generation of free phosphate was measured. Indeed, the HopAI1 protein displayed a potent activity in removing the phosphate group from the phosphopeptide (Figure S7).

In a separate study, we found that *Shigella flexneri* effector OspF targets animal MAPKs ERK1/2, JNK, and P38 (Li et al., 2007). Unlike protein phosphatases that remove the phosphate group at the CO-P bond, OspF is an enzyme that specifically cleaves the C-OP bond on phosphothreonine of ERK2 TXY motif. We named this novel enzyme as phosphothreonine lyases. The HopAI1 protein appears to have similar activity toward ERK2 synthetic phosphopeptide. We therefore tested if HopAI1 possesses phosphothreonine lyase activity toward plant MAPK peptide. The synthetic phosphopeptide corresponding to the MPK6 TXY motif was incubated with HopAI1, and the products were subjected to tandem mass spectrum analysis. The HopAI1 treatment reduced

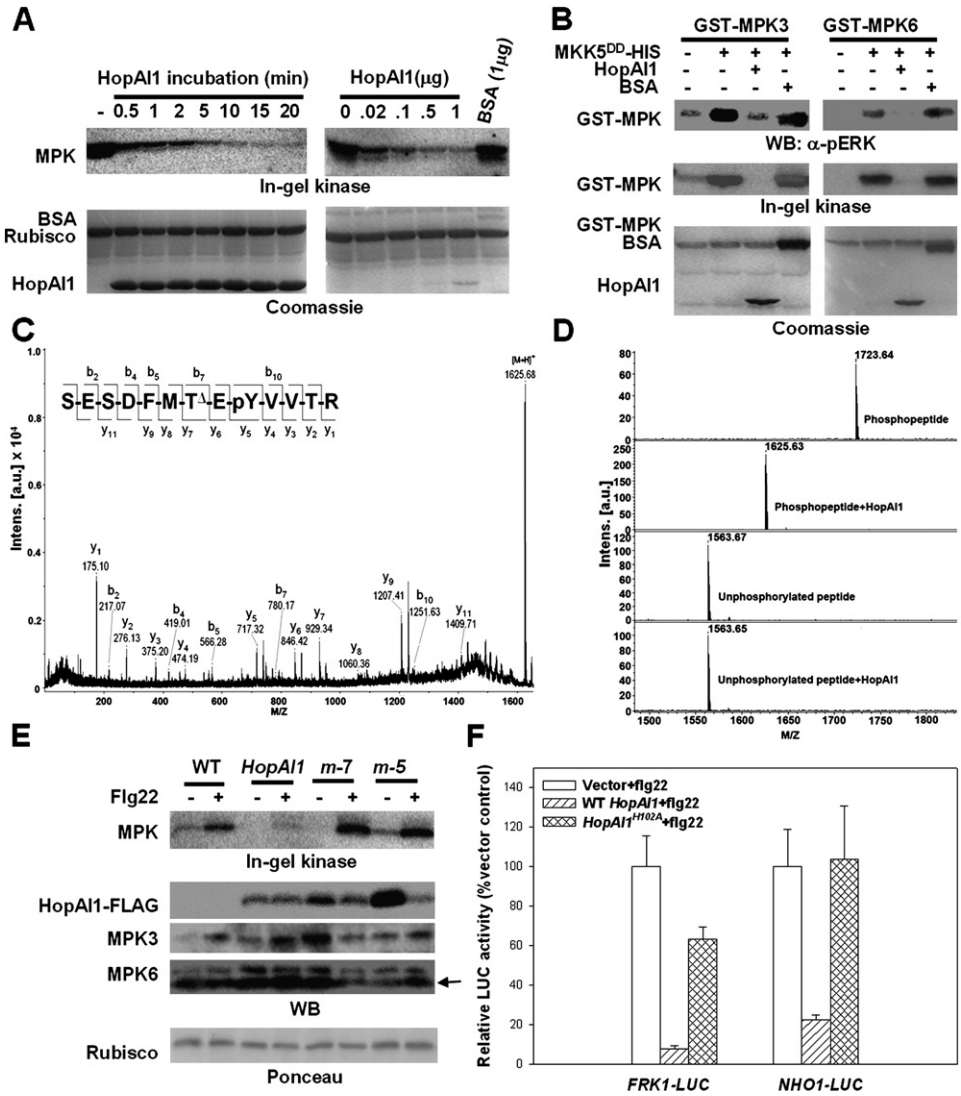

Figure 5. Purified HopAI1 Inactivates MPK3 and MPK6 by Dephosphorylation

(A) Left: total protein extract from flg22-induced WT plants was incubated with 10 μg purifed recombinant HopAI1$^{7-245}$ protein for the indicated times before in-gel kinase assay. Right: the extract was incubated with indicated amounts of HopAI1$^{7-245}$ or BSA for 20 min before in-gel kinase assay.

(B) HopAI1 dephosphorylates MPK3 and MPK6 in vitro. Purified GST-MPK3 and GST-MPK6 were phosphorylated with MKK5^{DD}-His. The reaction was terminated by adding 10 mM EDTA before incubated with purified HopAI1$^{7-245}$ or BSA. Amounts of MAPK phosphorylation were detected with anti-pERK antibodies. The dephosphorylated MAPKs were also subject to in-gel kinase assay. The amounts of GST-MPK and HopAI1 protein were indicated by Ponceau S staining.

(C) HopAI1 is a phosphothreonine lyase. The HopAI1$^{7-245}$-treated synthetic MPK6 phosphopeptide (SESDFM-pT-E-pYVVTR) was analyzed by tandem mass spectrometry. The fragmentation profile was indicated by the b and y ions. T$^{\Delta}$ in the indicated peptide sequence denotes the modification as a result of the treatment.

(D) The enzymatic activity of HopAI1 is specific to phosphorylated MPK6 peptide. Phosphorylated and unphosphorylated peptides were treated with HopAI1$^{7-245}$, and the mass of the resulting peptides was compared with untreated peptides by mass spectrometry.

(E) HopAI1^{His102Ala} does not inhibit MAPK activation. Two independent transgenic lines carrying FLAG-tagged *HopAI1*^{His102Ala} (m-5 and m-7) in the T1 generation were induced by estradiol, treated with flg22 peptide, and MAPK activity was compared with that in WT and transgenic plants expressing the WT HopAI1. The amounts of HopAI1-FLAG, MPK3, and MPK6 (arrow) protein were determined with the indicated antibodies. A representative protein blot was stained with Ponceau S to show equal loading of protein.

(F) The conserved amino acid required for phosphothreonine lyase activity is necessary for HopAI1 to suppress flg22-induced gene expression. Protoplasts prepared from WT plants were cotransfected with the *FRK1-LUC* reporter construct and WT *HopAI1*, *HopAI1*^{His102Ala} or an empty vector. Protoplasts prepared from *NHO1-LUC* transgenic plants were transfected with WT *HopAI1*, *HopAI1*^{His102Ala} or an empty vector. The transfected protoplasts were induced with flg22 for 3 hr for *FRK1-LUC* and 6 hr for *NHO1-LUC* before the *LUC* activity was determined.

the mass of phosphothreonine from 181 Da to 83 Da (Figure 5C). In contrast, the phosphotyrosine residue is not modified by HopAI1, indicating that HopAI1 specifically cleaves the C-OP bond of phosphothreonine of the MPK6 peptide. To determine if HopAI1 also removes the hydroxyl group of unphosphorylated threonine, a synthetic unphosphorylated MPK6 peptide was incubated with HopAI1, and mass spectrometry was used to determine the mass of the product. While the HopAI1 treatment reduced the phosphopeptide by 98 dalton, the same treatment did not alter the unphosphorylated peptide (Figure 5D). Thus, the enzymatic activity was specific to phosphothreonine, but not unphosphorylated threonine.

HopAI1 Phosphothreonine Lyase Activity Is Required for Defense Inhibition

The conserved histidine residue (OspF^{His104}) was found to be required for the enzymatic activity of OspF (Li et al., 2007). To test if this residue is required for the function of HopAI1, we introduced a corresponding mutation (His102Ala) into HopAI1 and tested transgenic plants expressing HopAI1^{His102Ala}. Two independent transgenic lines were tested for MAPK activation in response to flg22. As expected, both mutant lines showed nearly normal MAPK activation (Figure 5E). We further tested if this residue is required for HopAI1 to inhibit flg22-induced gene expression in protoplasts. As shown in Figure 5F, while the WT HopAI1 diminished the expression of *FRK1-LUC* to 8% of the control and *NHO1-LUC* to 22% of the control, the HopAI1^{His102Ala} mutant only slightly reduced the expression of *FRK1-LUC* (62% of the control) and has no effect on *NHO1-LUC* expression. These results indicate that the phosphothreonine lyase activity is required for HopAI1 to suppress flg22-induced defenses.

DISCUSSION

Earlier reports have provided controversial results concerning the role of the HopAI1 family effectors on MAPK signaling (He et al., 2006; Zurawski et al., 2006). In this study, we systematically determined the role of HopAI1 in defense suppression and its biochemical function. This led to the identification of MPK3 and MPK6 as its targets. HopAI1 inhibits flg22-induced immunity by directly dephosphorylating MPK3 and MPK6. Whether HopAI1 also inhibits other *Arabidopsis* MAPKs remains to be determined. Following the submission of this paper, Arbibe et al. (2007) reported that OspF acts as a protein phosphatase to dephosphorylate animal MAPKs. However, the HopAI1 family effectors do not share remote similarity with known protein phosphatases. Protein structural study indicated that SpvC does not carry any known phosphatase fold (L.C., H. Wang, and J.C., unpublished data). As demonstrated in Figure 5 and Li et al. (2007), the HopAI1 family effectors inactivate MAPKs through their phosphothreonine lyase activity, underscoring a new mechanism by which pathogenic bacteria promote virulence. The requirement of a phosphorylated threonine suggests that HopAI1 protein only attacks the C-O bond weakened by the phosphate group. The fundamental difference between this new enzyme and protein phosphatases is that the former results in a threonine residue lacking the hydroxyl group, preventing the rephosphorylation of MAPKs. Indeed, OspF-treated animal MAPKs was not rephosphorylated by MEK (Li et al., 2007).

P. syringae carries a large number of type III effectors. However, little is known about how these effectors promote virulence in the plant cell. The *Arabidopsis* adenosine diphosphate ribosylation factor guanine nucleotide exchange factor AtMIN7 is the only plant protein known to be targeted by a bacterial effector for virulence (Nomura et al., 2006). In *Arabidopsis*, *P. syringae* effectors AvrPto and AvrPtoB are able to inhibit MAPK signaling pathway, but their targets and mechanism remain unknown (He et al., 2006). Another *P. syringae* effector, HopD2, is a tyrosine phosphatase that is similar to the *Yersinia* effector YopH (Bretz et al., 2003; Espinosa et al., 2003). However, this effector was shown not to inhibit MPK3 and MPK6 (He et al., 2006), and its host target remains unknown. The work described here shows that HopAI1 plays an important role in bacterial virulence by directly targeting MAPKs, re-enforcing the notion that MAPK activation is central to plant PAMP-induced immunity. The use of HopAI1 transgenic plants led to the identification of the novel biochemical function of this effector. HopAI1 inactivates MAPKs through an unconventional phosphothreonine lyase activity unique to bacterial effectors, underscoring an ingenious strategy evolved in bacteria to modulate host defense signaling.

The regulation and role of the transient oxidative burst in PAMP-induced plant defenses had been unclear. ROIs generated during plant-pathogen interactions are thought to act as a secondary signal to regulate a diverse array of plant responses including Ca^{2+} influx, hypersensitive response, MAPK activation, and defense gene induction (Doke, 1983; Jabs et al., 1996; Mori and Schroeder, 2004; Torres and Dangl, 2005). Recent studies suggested a complex interaction between the MAPK pathway and *rboh*-dependent ROI production (Desikan et al., 2001; Samuel and Ellis, 2002; Rentel et al., 2004). Although it is possible that HopAI1 may inactivate phosphorylated proteins in addition to MAPKs, the most plausible interpretation of the data is that MAPKs act upstream of the AtrbohD-dependent ROI production during PAMP signaling. This is consistent with an earlier study indicating that activation of MAPK by the constitutive active MKK5^{DD} mutant results in H_2O_2 production (Ren et al., 2002). The AtrbohD-dependent ROI may trigger callose deposition by regulating either the biosynthesis or deposition of (1→3) β-D-glucan at the cell wall.

We propose a model illustrating how HopAI1 suppresses PAMP-induced immunity (Figure 6). Upon the perception of PAMPs, MPK3 and MPK6 are activated to regulate two downstream pathways important for disease resistance, the transcription of a large number of genes and callose deposition. The former is probably mediated by transcription factors such as WRKY22 and WRKY29 (Asai et al., 2002), whereas the latter is synthesized by callose

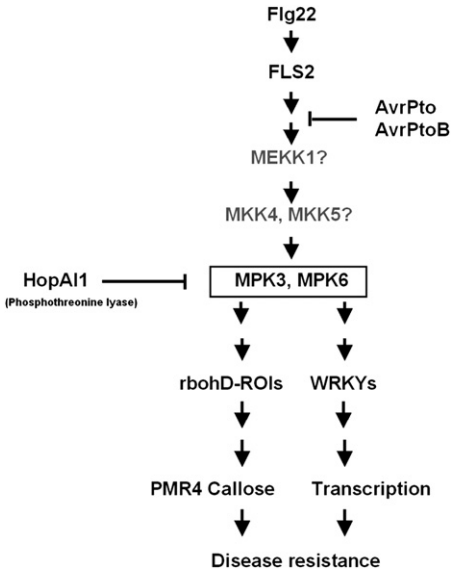

Figure 6. Model for HopAI1 Function and PAMP-Induced Signaling Pathway

The perception of flg22 by the receptor FLS2 activates MPK3 and MPK6 that subsequently phosphorylate the yet to be identified substrates to activate WRKY-mediated gene transcription and AtrbohD-mediated ROI production and cell wall defenses. HopAI1 binds and dephosphorylates MAPKs through its phosphothreonine lyase activity, and subsequently inhibits down-stream defense responses. Two previously reported effectors, AvrPto and AvrPtoB, target an unknown component(s) upstream of the MAPK cascade. FLS2 may also activate downstream signaling through a MAPK-independent pathway not shown in the model (He et al., 2006).

synthase PMR4 (Nishimura et al., 2003; Jacobs et al., 2003) and regulated by the AtrbohD-dependent ROI production. MKK4, MKK5, and MEKK1 were proposed to operate upstream of MPK3 and MPK6 (Asai et al., 2002), but such a role has yet to be supported by genetic data (Ichimura et al., 2006). HopAI1 directly dephosphorylates MAPKs through its phosphothreonine lyase activity, thereby inactivating MPK3 and MPK6 and suppressing both PAMP-induced gene transcription and the cell wall defense.

EXPERIMENTAL PROCEDURES

Plants and Bacterial Strains

Arabidopsis thaliana plants used in this study include the wild-type (Col-0), the *atrbohD* and *atrbohF* mutants (Torres et al., 2002), the T-DNA insertional mutants *atmpk6* and *atmpk3* (a gift from Shuqun Zhang; Liu and Zhang, 2004), a fast-neutron generated *atmpk3* deletion mutant (a gift from Yuelin Zhang), a dexamethasone-inducible $MKK5^{DD}$ transgenic line (Liu and Zhang, 2004), and *HopAI1-FLAG* transgenic plants (Li et al., 2005). To generate $HopAI1^{His102Ala}$*-FLAG* transgenic plants, a $HopAI1^{His102Ala}$ mutation was introduced into the *HopAI1-FLAG* construct, and the resulting mutant was introduced into Col-0 plants by Agrobacterium-mediated transformation according to standard protocols. Tomato cultivar PtoS used for bacterial growth assays is susceptible to *P.s.* pv. *tomato* bacteria.

Pseudomonas strains *P.s.* pv. *tomato* T1, *P.s.* pv. *tabaci* R1152 race 0, *P.s.* pv. *tomato* DC3000, *P.s.* pv. *maculicola* 4326, *P.s.* pv. *phaseolicola* NPS3121, *P.s.* pv. *glycinea* race 0, *P.s.* pv. *syringae* 3525, *P.s.* pv. *phaseolicola* PP14, *P.s.* pv. *syringae* UW25 race 1, *P.s.* pv. *phaseolicola* UW275 race 1, *P. cichorii* 72-4, *P. cichorii* 72-23, *P. cichorii* 74-1, and *P. cichorii* 74-4 were as described in previous studies (Davis et al., 1991; Kang et al., 2003). *P.s.* pv. *tomato* 0288-9, *P.s.* pv. *tomato* 1087-2, *P.s.* pv. *tomato* 1287-7, *P.s.* pv. *tomato* 0887-6, *P.s.* pv. *tomato* 0489-5, *P.s.* pv. *tomato* 0482-1, *P.s.* pv. *tomato* 0682-7, *P.s.* pv. *tomato* 0488-5, *P.s.* pv. *tomato* 0183-1, *P.s.* pv. *tomato* 0683-23, *P.s.* pv. *tomato* 0893-7, and *P.s.* pv. *tomato* 0483-16 were a gift from Carol Bender. To generate *hopAI1* knockout mutant, a truncated *hopAI1* coding sequence was PCR amplified using primers 5′-TGCGT GCTCATACACCGAC-3′and 5′-AGACGCATACGCCCAGTGAC-3′ and inserted into the PCR2.1-TOPO vector (Invitrogen). The resulting plasmid was introduced into strain 0288-9, and kanamycin resistant clones were verified by PCR for successful recombination. The resulting mutant carries a truncated *hopAI1* gene lacking the promoter sequence and the N-terminal 35 amino acids required for type III secretion and a second copy of *hopAI1* gene lacking the C-terminal 57 amino acids.

Oxidative Burst

Untreated or estradiol-induced leaves were sliced into approximately 1 mm strips, incubated in H_2O in a 24 well plate for 12 hr, and equal amounts of leaf tissues were treated with 1 μM flg22 in 500 μl buffer containing 20 μM luminol and 1 μg horseradish peroxidase (Sigma). Luminescence was recorded for 20 min by using a low-light imaging system, and relative luminescence was calculated with the WINVIEW software (Roper Scientific).

Flg22-Protection Assay

Five-week-old plants were first infiltrated with 1 μM flg22 or H_2O one day before infiltrating 10^5 CFU/ml *P. syringae* DC3000. Leaf bacterial population was determined at the indicated times. In experiments involving transgenic plants carrying the *HopAI1* transgene, plants were presprayed with 50 μM estradiol for 12 hr before the flg22 infiltration. Leaf bacterial number was determined at the indicated times after bacterial inoculation. Each data point consisted of at least four replicates.

Callose Staining

Five-week-old *Arabidopsis* leaves were untreated or presprayed with 50 μM estradiol or H_2O 12 hr prior to the infiltration of 40 μM flg22. Leaves were removed 12 hr after infiltration, cleared, stained with aniline blue (Hauck et al., 2003), and mounted in 50% glycerol, and epifluorescence was visualized with a fluorescence microscope under ultraviolet light. The number of callose deposits per microscopic field of 0.1 mm^2 was calculated from six leaves by using the Image J software (http://www.uhnresearch.ca/wcif).

MAPK Assay

The ΔMEKK1 construct was made by PCR amplifying the kinase catalytic domain from amino acids 326 to 592 (Asai et al., 2002) using primers 5′-AATGGATCCATGGGAGGAGCTATCATAACGTCTTG-3′ and 5′-ACTGGTCGACTCATGGTAAGGGTCTTCTCACAAATG-3′. The resulting PCR product was inserted into pUC19-35S-FLAG-RBS plasmid (Li et al., 2005) predigested with *BamH*I and *Cla*I. The $MKK5^{DD}$ construct for protoplast expression was made by PCR amplifying the pET28-$MKK5^{DD}$ plasmid (Liu and Zhang, 2004) and inserted between *Xho*I and *Csp*45I of the pUC19-35S-FLAG-RBS plasmid. The *HopAI1* and *AvrPto* constructs used for transient expression were described previously (Li et al., 2005). Protoplasts were isolated from 6-week-old plants and transfected with desired constructs according to a protocol developed by the Sheen lab (http://www.genetics.mgh.harvard.edu_sheenweb). Transfected protoplasts were incubated for 6 hr, and 1 μM flg22 or H_2O was added for 10 min before protein was extracted for in-gel kinase assay as described (Zhang and Klessig, 1997). For MAPK assay with leaf tissues, 5-week-old plants were sprayed with 10 μM flg22 or H_2O containing 0.02% Silwet L-77 for 10 min before protein extraction. Ten micrograms of total protein from leaves or protoplasts was electrophoresed on 12% SDS-polyacrylamide gels embedded with 0.25 mg/ml of myelin basic protein (MBP) in the separating gel as a substrate for the kinase.

The level of HopAI1-FLAG, AvrPto, MPK3, and MPK6 proteins in the extracts was determined by western blot analysis using anti-AvrPto (Shan et al., 2000), anti-FLAG, anti-MPK3, or anti-MPK6 antibodies (Sigma).

RNA Blot Analysis

Flg22-inducible genes were selected according to microarray data deposited by T. Nürnberger (http://Arabidopsis.org/info/expression/ATGenExpress.jsp). Gene specific primers were used to amplify *WRKY22*, *WRKY29*, *FRK1* (Asai et al., 2002), *At1g13110*(5′-TGAGATGCTAGTCGCTGGTG-3′, 5′-TGAACAAGTGGAACAAGCTC-3′), *At1g30700*(5′-TGGAGGTTACGGTAACATG-3′, 5′-ACACAGGAATACTCTGTTCG-3′), *At2g35930*(5′-AGCAGGGATATGCAAGAATC-3′, 5′-ACATCGTAAGCAACGACTC-3′), *At2g39200*(5′-TCAACCTTGACATGCTCAAC-3′, 5′-AGGAGATGTGGTTAAAGGAG-3′), *At2g44370*(5′-ACTTGAGACAAGCCTTTCTC-3′, 5′-ACCATCCATTGCGCAGTCAC-3′), *At5g39580*(5′-AACCGCAGAGCAAACCCTAC-3′, 5′-TGTCTCTTGTGCTGATATC-3′), and *At5g44910*(5′-ATTGAGAGACGAGAGAGTC-3′, 5′-ACAGTAAAGCTGGTGCAAG-3′). Five-week-old plants were infiltrated with H_2O or 1 μM flg22 for the indicated hours before RNA isolation. RNA blots were hybridized to radio-labeled PCR products for the selected genes.

Expression of Recombinant Proteins in *E. coli* and Protein Pull-Down Assay

Full length *Arabidopsis* MPK3 and MPK6 were PCR amplified from cDNA and inserted between the *BamH*I and *Xho*I sites of pGEX-6p-1 (Pharmacia) to generate GST-MPK3, GST-MPK6, and *Nde*I and *Xho*I of pET28b or pET30a (Novagen) to generate His-MPK3 and MPK6-His constructs. HopAI1$^{7-245}$ was PCR-amplified from *P. syringae* DC3000 genomic DNA and inserted into pGEX-6p-1 plasmid (between *BamH*I and *Xho*I) to generate GST- HopAI1$^{7-245}$. The respective recombinant proteins were affinity purified following manufactures' instructions.

For protein pull-down assay, His-MPK3 and MPK6-His were coexpressed with GST- HopAI1$^{7-245}$. Bacterial lysate was incubated with glutathione agarose in a microcentrifuge tube, washed three times with a buffer containing 25 mM Tris, PH8.0, 50 mM NaCL, and 3 mM DTT. The bound protein was eluted with 15 mM GSH and analyzed by using western blot.

Coimmunoprecipitation Assay

Five-week old plants were sprayed with 50 μM estradiol for 12 hr. Soluble protein was extracted and precipitated with an agarose-conjugated anti-FLAG monoclonal antibody (Sigma) following manufacturer's instruction. Western blot was used to detect the presence of HopAI1-FLAG, MPK3, or MPK6 in the immunocomplex with a monoclonal anti-FLAG antibody, or anti-MPK3 or anti-MPK6 antibodies (Sigma).

Reporter Assay in Protoplasts

Protoplasts were prepared from 6-week-old WT or *NHO1-LUC* transgenic plants (Li et al., 2005), transfected with the indicated plasmids, induced with flg22, and examined for LUC activity as described (Li et al., 2005).

MAPK Phosphorylation and Inactivation In Vitro

0.5 μg purified MKK5^{DD}-His recombinant protein was incubated with 2 μg GST-MPK3 or GST-MPK6 in a kinase reaction buffer (Liu and Zhang, 2004) at 22°C for 90 min before terminated by the addition of 10 mM EDTA. The phosphorylated GST-MPK3 and GST-MPK6 proteins were incubated with 5 μg purified HopAI1$^{7-245}$ or BSA for 10 min, boiled in SDS sample buffer before analyzed by using western blot with anti-phospho-ERK antibodies (Cell Signaling).

Phosphothreonine Lyase Activity Assays

Synthetic MAPK phosphopeptide (SESDFM-pTE-pYVVTR; Sangon, Shanghai) was incubated with 5 μg HopAI1$^{7-245}$ in a 50 μl reaction buffer containing 10 mM HEPES (pH 7.4), 150 mM NaCl, and 1 mM EDTA and incubated at 30°C, and the release of phosphate group was determined by using Molybdate Dye (Promega). The specific modification of phosphothreonine residue in the HopAI1-treated peptide was determined by mass spectrometry and tandem mass spectrometry analyses.

Supplemental Data

The Supplemental Data include seven supplemental figures and can be found with this article online at http://www.cellhostandmicrobe.com/cgi/content/full/1/3/175/DC1/.

ACKNOWLEDGMENTS

The authors are grateful to Jonathan Jones for permission to use the *atrbohD* and *atrbohF* mutants, Shuqun Zhang and Yuelin Zhang for providing Arabidopsis mutants, Dongtao Ren for MKK5^{DD} constructs and transgenic seeds, and Carol Bender for *Pseudomonas* strains. J.-M.Z. was supported by a grant from Chinese Ministry of Science and Technology (2003-AA210080).

Received: October 29, 2006
Revised: January 28, 2007
Accepted: March 5, 2007
Published: May 16, 2007

REFERENCES

Alfano, J.R., and Collmer, A. (2004). Type III secretion system effector proteins: Double agents in bacterial disease and plant defense. Annu. Rev. Phytopathol. *42*, 385–414.

Arbibe, L., Kim, D.W., Batsche, E., Pedron, T., Bogdan Mateescu, B., Christian Muchardt, C., Parsot, C., and Sansonetti, P.J. (2007). An injected bacterial effector targets chromatin access for transcription factor NF-κB to alter transcription of host genes involved in immune responses. Nat. Immunol. *8*, 47–56.

Asai, T., Tena, G., Plotnikova, J., Willmann, M.R., Chiu, W.-L., Gomez-Gomez, L., Boller, T., Ausubel, F.M., and Sheen, J. (2002). MAP kinase signaling cascade in *Arabidopsis* innate immunity. Nature *415*, 977–983.

Ausubel, F.M. (2005). Are innate immune signaling pathways in plants and animals conserved? Nat. Immunol. *6*, 973–979.

Axtell, M.J., and Staskawicz, B.J. (2003). Initiation of RPS2-specified disease resistance in Arabidopsis is coupled to the AvrRpt2-directed elimination of RIN4. Cell *112*, 369–377.

Boller, T. (1995). Chemoperception of microbial signals in plant cells. Annu. Rev. Plant Physiol. Plant Mol. Biol. *46*, 189–214.

Bretz, J.R., Mock, N.M., Charity, J.C., Zeyad, S., Baker, C.J., and Hutcheson, S.W. (2003). A translocated protein tyrosine phosphatase of Pseudomonas syringae pv. tomato DC3000 modulates plant defence response to infection. Mol. Microbiol. *49*, 389–400.

Chisholm, S.T., Coaker, G., Day, B., and Staskawicz, B.J. (2006). Host-microbe interactions: Shaping the evolution of the plant immune response. Cell *124*, 803–814.

Davis, K.R., Schott, E., and Ausubel, F.M. (1991). Virulence of selected phytopathogenic pseudomonads in *Arabidopsis thaliana*. Mol. Plant Microbe Interact. *4*, 477–488.

Desikan, R., Hancock, J.T., Ichimura, K., Shinozaki, K., and Neill, S.J. (2001). Harpin induces activation of the *Arabidopsis* mitogenactivated protein kinases AtMPK4 and AtMPK6. Plant Physiol. *126*, 1579–1587.

Doke, N. (1983). Involvement of superoxide anion generation in the hypersensitive response of potato tuber tissues to infection with an incompatible race of *Phytophthora infestans* and to the hyphal wall components. Physiol. Plant Pathol. *23*, 345–357.

Espinosa, A., Guo, M., Tam, V.C., Fu, Z.Q., and Alfano, J.R. (2003). The *Pseudomonas syringae* type III-secreted protein HopPtoD2 possesses protein tyrosine phosphatase activity and suppresses programmed cell death in plants. Mol. Microbiol. *49*, 377–387.

Felix, G., Duran, J.D., Volko, S., and Boller, T. (1999). Plants have a sensitive perception system for the most conserved domain of bacterial flagellin. Plant J. *18*, 265–276.

Gomez-Gomez, L., and Boller, T. (2000). FLS2: An LRR receptor-like kinase involved in the perception of the bacterial elicitor flagellin in *Arabidopsis*. Mol. Cell *5*, 1003–1011.

Gulig, P.A., and Chiodo, V.A. (1990). Genetic and DNA sequence analysis of the *Salmonella typhimurium* virulence plasmid gene encoding the 28,000-molecular-weight protein. Infect. Immun. *58*, 2651–2658.

Hauck, P., Thilmony, R., and He, S.Y. (2003). A *Pseudomonas syringae* type III effector suppresses cell wall-based extracellular defense in susceptible *Arabidopsis* plants. Proc. Natl. Acad. Sci. USA *100*, 8577–8582.

He, P., Shan, L., Lin, N.C., Martin, G.B., Kemmerling, B., Nürnberger, T., and Sheen, J. (2006). Specific Bacterial Suppressors of MAMP Signaling Upstream of MAPKKK in *Arabidopsis* Innate Immunity. Cell *125*, 563–575.

Ichimura, K., Casais, C., Peck, S.C., Shinozaki, K., and Shirasu, K. (2006). MEKK1 is required for MPK4 activation and regulates tissue specific and temperature dependent cell death in Arabidopsis. J. Biol. Chem. *281*, 36969–36976. Published online October 5, 2006. 10.1074/jbc.M605319200.

Jabs, T., Dietrich, R.A., and Dangl, J.L. (1996). Initiation of runaway cell death in an *Arabidopsis* mutant by extracellular superoxide. Science *273*, 1853–1856.

Jacobs, A.K., Lipka, V., Burton, R.A., Panstruga, R., Strizhov, N., Schulze-Lefert, P., and Fincher, G.B. (2003). An *Arabidopsis* callose synthase, *GSL5*, is required for wound and papillary callose formation. Plant Cell *15*, 2503–2513.

Kang, L., Li, J., Zhao, T., Xiao, F., Tang, X., Thilmony, R., He, S., and Zhou, J.M. (2003). Interplay of the Arabidopsis nonhost resistance gene NHO1 with bacterial virulence. Proc. Natl. Acad. Sci. USA *100*, 3519–3524.

Kim, M.G., da Cunha, L., McFall, A.J., Belkhadir, Y., DebRoy, S., Dangl, J.L., and Mackey, D. (2005). Two Pseudomonas syringae type III effectors inhibit RIN4-regulated basal defense in Arabidopsis. Cell *121*, 749–759.

Kovtun, Y., Chiu, W.L., Tena, G., and Sheen, J. (2000). Functional analysis of oxidative stress-activated mitogen-activated protein kinase cascade in plants. Proc. Natl. Acad. Sci. USA *97*, 2940–2945.

Li, H., Xu, H., Zhou, Y., Zhang, J., Long, C., Li, S., Chen, S., Zhou, J.M., and Shao, F. (2007). The phosphothreonine lyase activity of a bacterial type III effector family. Science *315*, 1000–1003.

Li, X., Lin, H., Zhang, W., Zou, Y., Zhang, J., Tang, X., and Zhou, J.M. (2005). Flagellin induces innate immunity in nonhost interactions that is suppressed by *Pseudomonas syringae* effectors. Proc. Natl. Acad. Sci. USA *102*, 12990–12995.

Liu, Y., and Zhang, S. (2004). Phosphorylation of 1-aminocyclopropane-1-carboxylic acid synthase by MPK6, a stress-responsive mitogen-activated protein kinase, induces ethylene biosynthesis in *Arabidopsis*. Plant Cell *16*, 3386–3399.

Lindeberg, M., Cartinhour, S., Myers, C.R., Schechter, L.M., Schneider, D.J., and Collmer, A. (2006). Closing the circle on the discovery of genes encoding Hrp regulon members and Type III Secretion System effectors in the genomes of three model *Pseudomonas syringae* strains. Mol. Plant Microbe Interact. *19*, 1151–1158.

Mackey, D., Belkhadir, Y., Alonso, J.M., Ecker, J.R., and Dangl, J.L. (2003). Arabidopsis RIN4 is a target of the type III virulence effector AvrRpt2 and modulates RPS2-mediated resistance. Cell *112*, 379–389.

Mackey, D., Holt, B.F., III, Wiig, A., and Dangl, J.L. (2002). RIN4 interacts with Pseudomonas syringae type III effector molecules and is required for RPM1-mediated resistance in Arabidopsis. Cell *108*, 743–754.

Mori, I.C., and Schroeder, J.I. (2004). Reactive oxygen species activation of plant Ca2+ channels. A signaling mechanism in polar growth, hormone transduction, stress signaling, and hypothetically mechanotransduction. Plant Physiol. *135*, 702–708.

Navarro, L., Zipfel, C., Rowland, O., Keller, I., Robatzek, S., Boller, T., and Jones, J.D.G. (2004). The transcriptional innate immune response to flg22. Interplay and overlap with *Avr* gene-dependent defense responses and bacterial pathogenesis. Plant Physiol. *135*, 1113–1128.

Nishimura, M.T., Stein, M., Hou, B.H., Vogel, J.P., Edwards, H., and Somerville, S.C. (2003). Loss of a callose synthase results in salicylic acid-dependent disease resistance. Science *301*, 969–972.

Nomura, K., DebRoy, S., Lee, Y.H., Pumplin, N., Jones, J., and He, S.Y. (2006). A bacterial virulence protein suppresses host immunity to cause plant disease. Science *313*, 220–223.

Nürnberger, T., and Lipka, V. (2005). Non-host resistance in plants: New insights into an old phenomenon. Mol. Plant Pathol. *6*, 335–354.

Ren, D.T., Yang, H.P., and Zhang, S.Q. (2002). Cell death mediated by MAPK is associated with hydrogen peroxide production in Arabidopsis. J. Biol. Chem. *277*, 559–565.

Rentel, M.C., Lecourieux, D., Ouaked, F., Usher, S.L., Petersen, L., Okamoto, H., Knight, H., Peck, S.C., Grierson, C.S., Hirt, H., and Knight, M.R. (2004). OXI1 kinase is necessary for oxidative burst-mediated signaling in *Arabidopsis*. Nature *427*, 858–861.

Samuel, M.A., and Ellis, B.E. (2002). Double jeopardy: Both overexpression and suppression of a redox-activated plant mitogen activated protein kinase render tobacco plants ozone sensitive. Plant Cell *14*, 2059–2069.

Shan, L., Thara, V.K., Martin, G.B., Zhou, J.M., and Tang, X. (2000). The pseudomonas AvrPto protein is differentially recognized by tomato and tobacco and is localized to the plant plasma membrane. Plant Cell *12*, 2323–2338.

Shao, F., Golstein, C., Ade, J., Stoutemyer, M., Dixon, J.E., and Innes, R.W. (2003). Cleavage of Arabidopsis PBS1 by a bacterial type III effector. Science *301*, 1230–1233.

Thilmony, R., Underwood, W., and He, S.Y. (2006). Genome-wide transcriptional analysis of the *Arabidopsis thaliana* interaction with the plant pathogen *Pseudomonas syringae* pv. *tomato* DC3000 and the human pathogen *Escherichia coli* O157:H7. Plant J. *46*, 34–53.

Torres, M.A., and Dangl, J.L. (2005). Functions of the respiratory burst oxidase in biotic interactions, abiotic stress and development. Curr. Opin. Plant Biol. *8*, 397–403.

Torres, M.A., Dangl, J.L., and Jones, J.D. (2002). *Arabidopsis* gp91phox homologues AtrbohD and AtrbohF are required for accumulation of reactive oxygen intermediates in the plant defense response. Proc. Natl. Acad. Sci. USA *99*, 517–522.

Torres, M.A., Jones, J.D., and Dangl, J.L. (2005). Pathogen-induced, NADPH oxidase-derived reactive oxygen intermediates suppress spread of cell death in *Arabidopsis thaliana*. Nat Genet. *37*, 1130–1134.

Torres, M.A., Jones, J.D., and Dangl, J.L. (2006). Reactive oxygen species signaling in response to pathogens. Plant Physiol. *141*, 373–378.

Vinatzer, B.A., Teitzel, G.M., Lee, M.-W., Jelenska, J., Hotton, S., Fairfax, K., Jenrette, J., and Greenberg, J.T. (2006). The type III effector repertoire of *Pseudomonas syringae* pv. *syringae* B728a and its role in survival and disease on host and non-host plants. Mol. Microbiol. *62*, 26–44.

Zhang, S., and Klessig, D.F. (1997). Salicylic acid activates a 48-kD MAP kinase in tobacco. Plant Cell *9*, 809–824.

Zipfel, C., and Felix, G. (2005). Plants and animals: A different taste for microbes? Curr. Opin. Plant Biol. *8*, 353–360.

Zipfel, C., Robatzek, S., Navarro, L., Oakeley, E.J., Jones, J.D., Felix, G., and Boller, T. (2004). Bacterial disease resistance in *Arabidopsis* through flagellin perception. Nature *428*, 764–767.

Zurawski, D.V., Mitsuhata, C., Mumy, K.L., McCormick, B.A., and Maurelli, A.T. (2006). OspF and OspC1 are *Shigella flexneri* type III secretion system effectors that are required for postinvasion aspects of virulence. Infect. Immun. *74*, 5964–5976.